FULL PAPER

Dalton
www.rsc.org/dalton

Metastable states associated with a change in the metal–metal bonding network of $(Mo^{V})_6$ polyoxoanions: a DFT study of $[(Mo_2{}^{V}O_4)_3(\mu_6\text{-}CO_3)(\mu\text{-}CO_3)_3(\mu\text{-}OH)_3]^{5-}$ †

Marie-Madeleine Rohmer * and Marc Bénard

Laboratoire de Chimie Quantique, UMR 7551, CNRS, Université Louis Pasteur, 4 rue Blaise Pascal, F-67000 Strasbourg, France. E-mail: benard@quantix.u-strasbg.fr

Received 16th April 2003, Accepted 9th July 2003
First published as an Advance Article on the web 5th August 2003

DFT calculations carried out on the recently characterized cluster ion $[(Mo_2{}^{V}O_4)_3(\mu_6\text{-}CO_3)(\mu\text{-}CO_3)_3(\mu\text{-}OH)_3]^{5-}$ (**1**) confirm the existence of three Mo–Mo bonds localized across the oxo ligands, with a strong alternation of the Mo–Mo distances (2.63/3.71 Å). The possibility of stabilizing a different organization of the metal–metal bond network is then investigated. A local energy minimum with high relative energy (+2.12 eV) is associated with the displacement of three metal–metal bonds across the hydroxo/carbonate bridging ligands. The six Mo–Mo distances are then equalized in the range 3.1/3.3 Å. The dimeric structure of **1** tied up by a network of six hydrogen bonds suggests the idea of a concerted displacement of the six protons along the H-bond pathways. Two equilibrium positions differing by the location of the Mo–Mo bonds are again characterized for this hypothetic isomer of **1**. The most stable of these states (+1.43 eV with respect to the ground state of **1**) is now associated with a network of relatively short Mo–Mo bonds (3.01 Å) *localized across the carbonate ligands*.

1 Introduction

The quest for metastable states, conformers or stable isomers associated with structural changes affecting the ground state of transition metal complexes is presently the subject of growing interest. In the case of sodium nitroprusside, in which the light induced changes in the crystal structure were detected first in 1977,[1] this interest was motivated in part by a possible link between the structural versatility of NO as a ligand and the recently unveiled role played by this molecule as a key physiological regulator.[2] More generally, the photoinduced versatility of molecules considered either at the individual scale or as crystalline materials, has potential technological importance in relation with the design of molecular switches or of high capacity storage devices. The light-induced isomers belonging to the family of transition metal complexes of NO and other diatomic (N_2) or triatomic (NO_2, SO_2, SCN,. . .) ligands has been the subject of considerable investigations in the domains of crystallography, spectroscopy, and quantum-chemical modelling. It appears from these studies, recently reviewed by Coppens *et al.*,[3] that the various minima characterized for these complexes should be assigned to different coordination positions (end-on, side-on, *iso*-end-on) of the ligand. In this particular case, the metastable states that could be characterized in relation with changes in the *metal–ligand* relative orientation have been termed "linkage isomers".[3] More complex molecular architectures involving several transition metal atoms are also susceptible to display distinct minima on the ground state potential energy surface by just reorganizing the distribution of the metal–metal bonds. This form of isomerism was investigated first by Rauchfuss *et al.* in cubane-like $Ru_4E_4Cp_4$ clusters (E = S, Se, Te) oxidized into dicationic species.[4,5] The neutral clusters can be viewed as nested dimers of $Ru_2E_2Cp_2$ butterfly moieties displaying each a single metal–metal bond and two bridging chalcogen atoms. A two-electron oxidation yields a mixed-valence Ru^{III}/Ru^{IV} cluster with a third, localized Ru–Ru bond. Low temperature ^{1}H NMR spectra evidenced changes affecting the metal framework, which were interpreted in terms of "mobile metal–metal bonds".[4] As soon as two metal sites can be distinguished by replacing for instance C_5H_5 by C_5Me_5, real isomers based exclusively on the relative positions of the M–M bonds can be characterized from low-temperature NMR spectroscopy.[5] This form of isomerism, termed "geometric isomerism" by Rauchfuss *et al.*,[5] is in fact relevant to the more general concept of "bond-stretch isomerism" defined by Stohrer and Hoffmann,[6] and later by Parkin,[7] in the sense that isomers retain the same atomic arrangement in the same molecular topography – the cubane cage – and differ only in the distance between the pairs of metal atoms displaying or not a localized bond.[8] Theoretical studies in polyoxometalate chemistry have also shown that the localization/delocalization duality of electron pairs in reduced polyoxoanions could lead to multiple energy minima and to bond-stretch isomerism.[8,9] The synthesis of new families of functionalized polyoxometalates with cyclic cores of Mo^{V} and localized Mo–Mo bonds, initiated by Haushalter and Lai[10] and recently developed by several groups[11–13] raises questions about the potentialities offered by a reorganization of the metal–metal bonding network. The calculations reported here on the cluster $[(Mo_2{}^{V}O_4)_3(\mu_6\text{-}CO_3)(\mu\text{-}CO_3)_3(\mu\text{-}OH)_3]^{5-}$ (**1**), recently characterized by Manos *et al.*,[14] suggest that high energy metastable, or even stable states, associated with the changes in the metal–metal bond network, should exist on the potential energy surface of **1** and of similar molecules.

2 Computational details

All calculations have been carried out using the formalism of the Density Functional Theory (DFT) within the Generalized Gradient Approximation (GGA), as implemented in the ADF program.[15] The formalism is based upon the local spin density approximation characterized by the electron gas exchange ($X\alpha$ with α = 2/3) together with Vosko–Wilk–Nusair[16] parametrization for correlation. Nonlocal corrections due to Becke for the exchange energy[17] and to Perdew for the correlation energy[18] have been added. Most results reported in this work have been obtained by means of the Slater basis sets referred to as IV in the ADF User's Guide.[15a] For first row atoms, the 1s shell was frozen and described by a single Slater function. The frozen core of the Mo atoms composed of the 1s to 3sp shells was also modelled by a minimal Slater basis. For hydrogen, carbon and oxygen, the Slater basis set used for the valence shell

† Electronic supplementary information (ESI) available: bond energies and Cartesian coordinates of the four energy minima. See http://www.rsc.org/suppdata/dt/b3/b304119k/

DOI: 10.1039/b304119k

is of triple-ζ quality, supplemented with one p- or d-type polarization function.[19] The 4s and 4p shells of molybdenum are described by a double-ζ Slater basis; the 4d and 5s shells by a triple-ζ basis and the 5p shell by a single orbital. Basis set IV does not include polarization functions on the metal atoms and relativistic effects have not been taken into account. However, the geometry of the ground state of **1** and that of one of the investigated metastable states were reoptimized with Slater basis sets including one f-type function on metal atoms and accounting for quasirelativistic corrections for the core electrons. All calculations have been carried out with the constraints of the C_s symmetry point group, but the optimized structures never significantly deviate from the expected threefold symmetry. The geometry optimization processes have been carried out by minimizing the energy gradient by the BFGS formalism[20] combined with a DIIS-type convergence acceleration method.[21] The optimization cycles were continued until all of the three following convergence criteria were fulfilled: (i) the difference in the *total energy* between two successive cycles is less than 0.001 E_h; (ii) the difference in the *norm of the gradient* between two successive cycles is less than 0.001 E_h Å^{-1}; (iii) the maximal difference in the *Cartesian coordinates* between two successive cycles is less than 0.01 Å.

3 Results and discussion

3.1 Conformations optimized for complex 1

The structure of the $[(Mo_2{}^{V}O_4)_3(\mu_6\text{-}CO_3)(\mu\text{-}CO_3)_3(\mu\text{-}OH)_3]^{5-}$ ion, assumed isolated, has been optimized starting from two distinct trial geometries. Trial geometry I reproduces the structure of the polyoxoanion as obtained from the X-ray diffraction study of the $(NH_4)_5[(Mo_2{}^{V}O_4)_3(\mu_6\text{-}CO_3)(\mu\text{-}CO_3)_3(\mu\text{-}OH)_3]\cdot 0.5CH_3OH$ crystal.[14] This structure is characterized by an alternation of short and long Mo–Mo distances, the short contacts, such as Mo(1)–Mo(2) (2.588 Å) joining metal centers coordinated to two μ-oxo bridges, and the long ones, such as Mo(2)–Mo(3) (3.548 Å) separating Mo atoms coordinated each to an external carbonate bridge and to a hydroxo ligand (Fig. 1). Although the optimized bonding distances do not deviate much from the X-ray diffraction results (Table 1), the calculated structure of the cluster is somewhat expanded, a trend that can be explained by the tendency of GGA functionals to slightly overestimate bond lengths, and also by the high negative charge of the cluster, not compensated by the presence of counterions. The most significant deviation with respect to the crystal structure concerns the long Mo–Mo contacts, calculated to be 0.16 Å larger than experiment (Table 1). Inclusion of polarization functions on the metal atoms slightly improves the calculated structure by reducing the equilibrium Mo–Mo distances, either short or long, by ~0.04 Å (Table 1). The

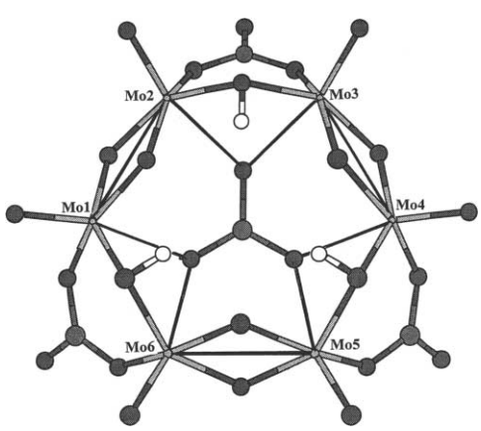

Fig. 1 XMOL view, down the three-fold axis of the $[(Mo_2{}^{V}O_4)_3(\mu_6\text{-}CO_3)(\mu\text{-}CO_3)_3(\mu\text{-}OH)_3]^{5-}$ ion. White circles represent hydrogen; light gray, molybdenum; darker gray, carbon and oxygen.

distribution of the frontier orbitals, characterized by a large HOMO–LUMO gap of 1.95 eV, confirms the presence of three localized bonds linking the metal atoms located in the edge-sharing octahedra (*i.e.* bridged by two oxo ligands; Fig. 2, above).

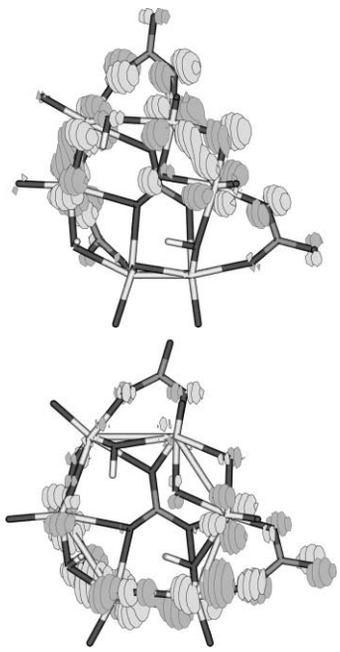

Fig. 2 The three highest occupied Kohn–Sham orbitals of $[(Mo_2{}^{V}O_4)_3(\mu_6\text{-}CO_3)(\mu\text{-}CO_3)_3(\mu\text{-}OH)_3]^{5-}$ (above) in the ground state conformation, and (below) in the metastable state resulting from the mobility of the metal–metal bonds.

Another trial geometry was then defined as a starting point for a new process of geometry optimization. Trial geometry II was derived from I by properly reversing the alternation of the metal–metal distances and roughly adapting the ligand environment to the modifications ascribed to the metal framework, *i.e.* keeping the metal–ligand distances to the values obtained from X-ray diffraction. In the course of the optimization process, the structure evolved rather far from the bond alternation defined in trial geometry II, but did not come back to – or close to – the conformation optimized first. The local energy minimum obtained from this second optimization process is relatively high-lying: +2.12 eV with respect to the global minimum, a value that is not significantly modified by the inclusion of f-type polarization functions. Contrary to our expectation, the change in the Mo–Mo distance alternation postulated in the trial geometry has not been retained in the local minimum. The lengths of the Mo(1)–Mo(2) axis bridged by the two oxo ligands as that of the hydroxocarbonate-bridged Mo(2)–Mo(3) axis have now the same order of magnitude, Mo(1)–Mo(2) still being shortest (3.133 *vs.* 3.294 Å, Table 1). However, an analysis of the three highest occupied Kohn–Sham orbitals confirms that the Mo–Mo bonds now span the carbonate bridges, whereas there is no more metal–metal interaction across the oxo bridges (Fig. 2, below).

In an attempt to locate the transition state and estimate the barrier height separating the high energy local minimum from the basin of the global energy minimum, a constrained optimization process was started with the Mo(1)–Mo(2) distance fixed at 2.95 Å. After a few optimization cycles, the calculation indefinitely oscillates between two positions characterized by large variations of the Mo(2)–Mo(3) distance (3.59 and 3.78 Å) and close energy values (−289.24 and −289.37 eV, respectively) both higher than the energy value of the metastable state, −289.55 eV (Table 1). This behaviour is interpreted as resulting from the oscillation of the Kohn–Sham orbitals between the configurations describing the two possible networks of metal–

Table 1 Selected distances (Å) in the experimental and in the four computed energy minima. Relative energies and HOMO–LUMO gaps are in eV

	Exp.	Form I[a]	Form II[b]	Form III[c]	Form IV[d]
Mo(1)–Mo(2)	2.588	2.629 (2.585)[e]	3.133 (3.092)[e]	2.820	3.330
Mo(2)–Mo(3)	3.548	3.708 (3.673)[e]	3.297 (3.211)[e]	3.523	3.007
μ-O ··· μ-O		2.92	2.44		
μ-O ··· μ-OH				3.01	2.40
Mo–(μ-O)	1.948	1.972	2.000	1.994[f] 1.989[g]	1.992[f] 1.966[g]
Mo–(μ-OH)	2.094	2.099	2.102	2.137	2.157
$Mo–O_{(\mu\text{-}CO3)}$	2.070	2.098	2.102	2.088	2.095
$Mo–O_{(\mu3\text{-}CO3)}$	2.355	2.404	2.367	2.371	2.363
$Mo–O_{terminal}$	1.674	1.750	1.752	1.748	1.752
Ω-Mo[h]		3.18	3.21	3.18	3.17
HOMO–LUMO gap		1.942	0.564	0.917	1.044
Relative energy		0.0	+2.12 (+2.13)[e]	+2.06	+1.43

[a] Conformation optimized using the X-ray structure as a trial geometry. [b] Conformation optimized from a trial geometry with opposite Mo–Mo distance alternation: in this trial geometry, Mo(2)–Mo(3), bridged by a carbonate ligand, is assigned the shortest distance. [c] Conformation optimized from a trial geometry in which the Mo–Mo bond alternation is the same as in form I, but the three protons have migrated from the hydroxo ligands to the oxo ligands facing them in the dimer. [d] Conformation optimized from a last trial geometry: Mo–Mo bond alternation as in form II, position of the protons as in form III. [e] Value obtained with a basis set including one f-type polarization function on metal atoms. [f] Oxygen facing the hydroxo ligand. [g] Oxygen facing the carbonate ligand. [h] Radius of the metal framework.

metal bonds, near the crossing point of the associated potential energy curves.

Should all contiguous pairs of metal atoms of the $(Mo^V)_6$ ring undergo the same ligand environment, then the two networks of metal–metal bonds would be associated with twin energy minima and with undistinguishable structures. The computed gap between the two energy minima of **1** therefore reflects the constraints imposed by the bridging ligands, either $(\mu\text{-}O)_2$ for Mo(1)–Mo(2), or (μ-OH, $\mu\text{-}CO_3$) for Mo(2)–Mo(3) and analogues. The electrostatic and Pauli repulsion induced by relatively close O ··· O contacts in Mo–$(\mu\text{-}O)_2$–Mo moieties penalizes structures with elongated Mo(1)–Mo(2) distances. The more flexible CO_3 ligand does not impose such severe a constraint on the metal–metal bond length. We therefore attribute to the imposed proximity of the oxo ligands the shift toward high energies of the isomer exhibiting carbonate-bridged Mo–Mo bonds. Indeed, the oxo ··· oxo distance in the high-energy isomer has decreased from 2.92 to 2.44 Å. The limitation of the stretching of the nonbonded Mo–Mo distances to 3.13 Å is therefore assigned to the rise of the repulsive interactions in the four-member rings. Conversely, the contraction of the Mo–Mo distance in the *bonded* moieties is limited to the rather high value of 3.29 Å by the necessity to maintain the optimal bond distances between the metal framework and the central carbonate. Table 1 shows that all optimized conformation are characterized by a near constancy of all metal–ligand distances as well as of the radius of the cyclic metal framework.

3.2 Transfer of the protons from (μ-OH) to (μ-O)

As most molybdenum compounds containing the planar, cyclic Mo^V_6 framework,[10–13] the $[(Mo_2{}^VO_4)_3(\mu_6\text{-}CO_3)(\mu\text{-}CO_3)_3(\mu\text{-}OH)_3]^{5-}$ ions are organized in dimers with a counterion at the center of the structure. In the present case, the connection between the monomers is strengthened by the presence of six hydrogen bonds connecting each a hydroxo ligand of one molecule to a bridging oxygen of the other monomer (Fig. 3). The existence of such a hydrogen bond network suggests another possibility of inducing the mobility of the metal–metal bonds at the expense of a minimal reorganization of the dimer topography and of the crystal structure. Let us assume a concerted displacement of the protons along the hydrogen bond pathway to the underlying oxo bridge (Fig. 4). This displacement by less than 1 Å of the six protons generates a dimeric anion in which the Pauli and electrostatic repulsion are partly transferred from the former oxo–oxo (now oxo–hydroxo) bridge to the oxo–carbonato bridge. The proposed conformation of the complex should therefore be less unfavorable to a concerted transfer of the metal electrons.

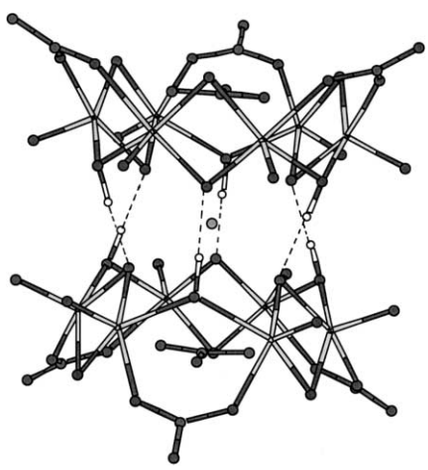

Fig. 3 XMOL view of the dimer of **1**, as observed in the crystal, showing the nitrogen atom of the central $(NH_4)^+$ counter-ion and the network of hydrogen bonds.

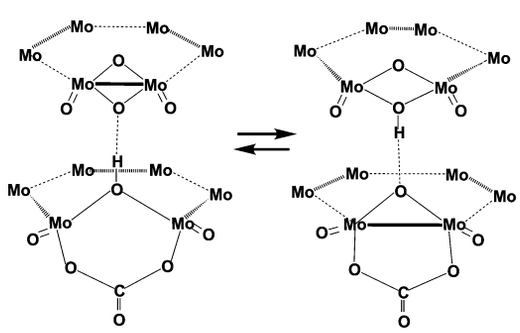

Fig. 4 Suggested pathway for a concerted transfer of the six protons inside the dimeric unit. The structure of the dimer is represented assuming the computed geometry of the monomer in the experimental conformation (left hand-side) and in the conformation of lowest energy resulting from the transfer of the protons (right hand-side). The separation observed between the hexanuclear metal frameworks has been assumed in both representations.

Calculations indeed confirm this assumption. Two equilibrium conformations for the isolated monomer are computed assuming the new protonation sites. These conformations,

referred to as III and IV, mainly differ by the relative positions of the metal atoms and are therefore reminiscent of forms I and II, respectively, calculated with the observed ligand arrangement (Table 1). In conformation III, the density accumulations associated with the three highest occupied orbitals are localized between the metal atom pairs separated by the oxo–hydroxo bridges. In form IV, these density accumulations are shifted to the pairs separated by the oxo–carbonato ligands. The relative energies of forms III and IV are however in striking contrast with the previous results since the latter distribution of the metal electrons is now the most stable one (Table 1). In III as in IV, the shortest metal–metal distances correspond to pairs of bonded atoms, which was not the case in form II. The calculated length of the metal–metal bond in IV is 3.007 Å, still much longer than the Mo–Mo distances of ~2.6 Å currently observed in such hexanuclear complexes.[10–14] Conversely, the nonbonded Mo–Mo separations (3.30 Å) are much shorter than observed, so that the radius of the cyclic metal framework remains remarkably constant in all four calculated equilibrium structures (Table 1). The long distances associated with the metal–metal bonds in IV suggest that the ligand–ligand repulsions remain somewhat unbalanced and prevent the system to take full advantage of the Mo–Mo bond network. Indeed, the energy associated with form IV exceeds by 1.43 eV that of the global minimum. This conformation, characterized by a reorganization of the metal–metal bond framework, seemingly represents the lowest *local* energy minimum accessible without implying a change in the topology of the centrosymmetric six-fold hydrogen bonded dimer.

4 Summary and conclusion

Calculations carried out on the $[(Mo_2^{V}O_4)_3(\mu_6\text{-}CO_3)(\mu\text{-}CO_3)_3(\mu\text{-}OH)_3]^{5-}$ ion (**1**) show that a substitute to the observed metal–metal bond network generates a local minimum on the ground state potential energy hypersurface. This local minimum could be associated with the existence of a metastable state, or possibly of a bond-stretch isomer with high energy. Indeed, the structural modifications induced by the concerted transfer of the metal electron density to the next pairs of metal atoms mainly affect the metal–metal distances, without modifying the ligand organization and the molecular topography. The radius of the cyclic framework itself remains remarkably constant, in probable relation with the structural constraint imposed by the central template. The structural change calculated in the planar Mo_6 framework is not reducible to a simple shift of the marked alternation observed in the metal–metal distances. The electrostatic and Pauli repulsion between two bridging oxo ligands prevents an important stretching of the Mo–Mo distance when the metal–metal bond is broken. All six metal–metal distances in the metastable state therefore lie in the narrow range 3.13–3.29 Å and the energy is raised by more than 2 eV. If we now consider the dimeric structure of the polyoxoanion in the crystal and the network of six hydrogen bonds connecting the two monomers, a concerted transfer of the six protons along the hydrogen bond pathways generates a new dimeric entity in which the rotation of the metal–metal bond system is now favored by 0.63 eV. It is clear that the qualitative conclusions deduced from the calculations carried out on **1** could be extended to the whole family of cyclic polyoxoanions containing six Mo^{V} atoms arranged in a planar framework, since this family appears quite homogeneous as far as the constraints of the molecular structure and the accommodation of the metal electrons are concerned.

Acknowledgements

We are pleased to thank IDRIS (Orsay, France) and CURRI (Strasbourg) for computer time allocations.

References

1 U. Hauser, V. Oestrekh and H. D. Rohrweck, *Z. Phys. A*, 1977, **280**(17), 125.
2 (*a*) G. B. Richter-Addo, P. Legzdins and J. Burstyn, *Chem. Rev.*, 2002, **102**, 857–860; (*b*) G. M. Rosen, P. Tsai and S. Pou, *Chem. Rev.*, 2002, **102**, 1191–1199; (*c*) L. J. Roman, P. Martásek and B. S. S. Masters, *Chem. Rev.*, 2002, **102**, 1179–1190.
3 P. Coppens, I. Novozhilova and A. Kovalevsky, *Chem. Rev.*, 2002, **102**, 861–863.
4 E. J. Houser, T. B. Rauchfuss and S. R. Wilson, *Inorg. Chem.*, 1993, **32**, 4069–4076.
5 Q. Feng, T. B. Rauchfuss and S. R. Wilson, *J. Am. Chem. Soc.*, 1995, **117**, 4702–4703.
6 W.-D. Stohrer and R. Hoffmann, *J. Am. Chem. Soc.*, 1972, **94**, 779–786; W.-D. Stohrer and R. Hoffmann, *J. Am. Chem. Soc.*, 1972, **94**, 1661–1668.
7 (*a*) G. Parkin, *Chem. Rev.*, 1993, **93**, 887–911; (*b*) G. Parkin, *Acc. Chem. Res.*, 1992, **25**, 455–460.
8 For a recent review on bond-stretch isomerism, see M.-M. Rohmer and M. Bénard, *Chem. Soc. Rev.*, 2001, **30**, 340–354.
9 M.-M. Rohmer, M. Bénard, E. Cadot and F. Sécheresse, *Polyoxometalate Chemistry; From Topology via Self-Assembly to Applications*, ed. M. T. Pope and A. Müller, Kluwer Academic Publishers, Dordrecht, The Netherlands, 2001, pp. 117–133.
10 (*a*) R. C. Haushalter and F. W. Lai, *Inorg. Chem.*, 1989, **28**, 2904–2905; (*b*) R. C. Haushalter and F. W. Lai, *Angew. Chem., Int. Ed. Engl.*, 1989, **28**, 743–746.
11 (*a*) A. Leclaire, A. Guesdon, F. Berrah, M. M. Borel and B. Raveau, *J. Solid. State Chem.*, 1999, **145**, 291–301; (*b*) A. Leclaire, C. Biot, H. Rebbah, M. M. Borel and B. Raveau, *J. Mater. Chem.*, 1998, **8**, 439–444; (*c*) A. Guesdon, M. M. Borel, A. Leclaire and B. Raveau, *Chem. Eur. J.*, 1997, **3**, 1797–1800; (*d*) P. Lightfoot and D. Masson, *Acta Crystallogr., Sect. C*, 1996, **52**, 1077; (*e*) P. Lightfoot and D. Masson, *Mater. Res. Bull.*, 1995, **30**, 1005; (*f*) L. A. Meyer and R. C. Haushalter, *Inorg. Chem.*, 1993, **32**, 1579–1586; (*g*) L. A. Mundi and R. C. Haushalter, *Inorg. Chem.*, 1992, **31**, 3050–3053.
12 (*a*) I. Khan, Q. Chen and J. Zubieta, *Inorg. Chim. Acta*, 1995, **235**, 135–145; (*b*) G. Cao, R. C. Haushalter and K. G. Strohmaier, *Inorg. Chem.*, 1993, **32**, 127–128; (*c*) I. Khan, Q. Chen and J. Zubieta, *Inorg. Chim. Acta*, 1993, **206**, 131–133; (*d*) Y.-D. Chang and J. Zubieta, *Inorg. Chim. Acta*, 1996, **245**, 177–198.
13 (*a*) E. Cadot, A. Dolbecq, B. Salignac and F. Sécheresse, *Chem. Eur. J.*, 1999, **5**, 2396–2403; (*b*) A. Dolbecq, E. Cadot and F. Sécheresse, *Chem. Commun.*, 1998, 2293–2295; (*c*) B. Salignac, S. Riedel, A. Dolbecq, F. Sécheresse and E. Cadot, *J. Am. Chem. Soc.*, 2000, **122**, 10381–10389.
14 M. J. Manos, A. D. Keramidas, J. D. Woollins, A. M. Z. Slawin and T. A. Kabanos, *J. Chem. Soc., Dalton Trans.*, 2001, 3419–3420.
15 (*a*) *ADF User's Guide, Release 1999*, Chemistry Department, Vrije Universiteit, Amsterdam, The Netherlands, 1999; (*b*) E. J. Baerends, D. E. Ellis and P. Ros, *Chem. Phys.*, 1973, **2**, 41–51; (*c*) G. te Velde and E. J. Baerends, *J. Comput. Phys.*, 1992, **99**, 84–98; (*d*) C. Fonseca-Guerra, O. Visser, J. G. Snijders, G. te Velde and E. J. Baerends, *Methods and Techniques in Computational Chemistry: METECC-95*, ed. E. Clementi and G. Corongiu, STEF, Cagliari, Italy, 1995, pp. 305–395.
16 S. H. Vosko, L. Wilk and M. Nusair, *Can. J. Phys.*, 1980, **58**, 1200–1211.
17 (*a*) A. D. Becke, *J. Chem. Phys.*, 1986, **84**, 4524–4529; (*b*) A. D. Becke, *Phys. Rev. A: At., Mol., Opt. Phys.*, 1988, **A38**, 3098–3100.
18 J. P. Perdew, *Phys. Rev.*, 1986, **B33**, 8822–8824.
19 (*a*) J. G. Snijders, E. J. Baerends and P. Vernooijs, *At. Nucl. Tables*, 1982, **26**, 483; (*b*) P. Vernooijs, J. G. Snijders and E. J. Baerends, Slater type basis functions for the whole periodic system, Internal Report, Free University of Amsterdam, The Netherlands, 1981.
20 T. H. Fisher and J. Almlöf, *J. Phys. Chem.*, 1992, **96**, 9768–9774.
21 L. Versluis, PhD Thesis, University of Calgary, Calgary, Alberta, Canada, 1989.